

ON DIVERSITY OF CONFIGURATIONS GENERATED BY EXCITABLE CELLULAR AUTOMATA WITH DYNAMICAL EXCITATION INTERVALS

ANDREW ADAMATZKY

ABSTRACT. Excitable cellular automata with dynamical excitation interval exhibit a wide range of space-time dynamics based on an interplay between propagating excitation patterns which modify excitability of the automaton cells. Such interactions leads to formation of standing domains of excitation, stationary waves and localised excitations. We analysed morphological and generative diversities of the functions studied and characterised the functions with highest values of the diversities. Amongst other intriguing discoveries we found that upper boundary of excitation interval more significantly affects morphological diversity of configurations generated than lower boundary of the interval does and there is no match between functions which produce configurations of excitation with highest morphological diversity and configurations of interval boundaries with highest morphological diversity. Potential directions of future studies of excitable media with dynamically changing excitability may focus on relations of the automaton model with living excitable media, e.g. neural tissue and muscles, novel materials with memristive properties, and networks of conductive polymers.

Keywords: excitation, automata, diversity, localisations, patter formation

1. INTRODUCTION

Since their popularisation in [5], excitable cellular automata became a convenient tool for studying complex phenomena of excitation dynamics and chemical reaction-diffusion activities in physical, chemical and biological systems [7, 3]. The cellular automata offers quick 'prototyping' of complex spatially extended non-linear media. The examples of 'best practice' include models of Belousov-Zhabotinsky reactions and other excitable systems [4, 8], chemical systems exhibiting Turing patterns [12, 9, 10], precipitating systems [2], calcium wave dynamics [11], and chemical turbulence [6].

In a classical Greenberg-Hasting [5] automaton model of excitation a cell takes three states — resetting, excited and refractory. A resting cell becomes excited if number of excited neighbours exceeds a certain threshold, an excited cell becomes refractory, and a refractory cell returns to its original resting state. In 1998 [1], we introduced an excitable cellular automaton, where a resting cell is excited if a number of its excited neighbours belongs to some fixed interval $[\theta_1, \theta_2]$. The interval $[\theta_1, \theta_2]$ was called an excitation interval. For a two-dimensional cellular automaton with eight-cell neighbourhood boundaries of the excitation interval satisfy the condition: $1 \leq \theta_1 \leq \theta_2 \leq 8$. We found that by tuning θ_1 and θ_2 we can force the automaton to imitate almost all kinds of excitation dynamics, from classical target and spiral waves observed in physical and chemical excitable media to wave-fragments inhabiting sub-excitable media.

How does excitation dynamics change if we allow boundaries of the excitation interval to change during the automaton development? We partially answer the question in present paper by making the interval $[\theta_1^t(x), \theta_2^t(x)]$ of every cell x to be dynamically updatable at every step t depending on state of the cell x and numbers of excited and refractory neighbours in the cell x 's neighbourhood.

The excitable automata with dynamical excitation intervals are defined in Sect. 2. Morphological diversity of cellular automata (measured using Shannon entropy and Simpson index) with different functions of interval updates is characterised in Sect. 3. Section 4 characterises generative diversity (measured in terms of different configurations generated during space-time development of automaton starting with a single non-resting cell) of the local transitions. Some afterthoughts are offered in Sect. 5.

2. DYNAMICAL EXCITATION INTERVALS

Let x^t and x^{t+1} be states of a cell x at time steps t and $t + 1$, and $\sigma_+^t(x)$ be a sum of excited neighbours in cell x 's neighbourhood $u(x) = \{y : |x - y|_{L_\infty} = 1\}$. Cell x updates its state by the following rule:

$$x^{t+1} = \begin{cases} +, & \text{if } x^t = \cdot \text{ and } \sigma_+^t(x) + \in [\theta_1^t(x), \theta_2^t(x)] \\ -, & \text{if } x^t = + \\ \cdot, & \text{otherwise} \end{cases}$$

A resting cell is excited if number of its neighbours belongs to excitation interval $[\theta_1^t(x), \theta_2^t(x)]$, where $1 \leq \theta_1^t(x), \theta_2^t(x) \leq 8$. The boundaries $\theta_1^t(x)$ and $\theta_2^t(x)$ are dynamically updated depending on cell x 's state and numbers of x 's excited $\sigma_+^t(x)$ and refractory $\sigma_-^t(x)$ neighbours. A natural way to update boundaries is by increasing or decreasing their values as follows:

$$\begin{aligned} \theta_1^{t+1}(x) &= \xi(\theta_1^t(x) + \Delta_1 \phi(\sigma_+^t(x) - \sigma_-^t(x))) \\ \theta_2^{t+1}(x) &= \xi(\theta_2^t(x) + \Delta_2 \phi(\sigma_+^t(x) - \sigma_-^t(x))) \end{aligned}$$

where

$$\Delta_1 = \begin{cases} T_1, & \text{if } x = + \\ T_3, & \text{if } x = - \\ 0, & \text{if } x = 0 \end{cases} \quad \Delta_2 = \begin{cases} T_2, & \text{if } x = + \\ T_4, & \text{if } x = - \\ 0, & \text{if } x = 0 \end{cases}$$

and $\phi(a - b) = 1$ if $a > b$, 0 if $a = b$ and -1 if $a < b$, and $\xi(a) = 1$ if $a < 1$ and 8 if $a > 8$. Boundaries of excitation interval $[\theta_1^t(x), \theta_2^t(x)]$ are updated independently of each other. Local excitation rules are determined by values of T_1, \dots, T_4 . We therefore address the functions as tuples $E(T_1 T_2 T_3 T_4)$ which range from $E(-1 - 1 - 1 - 1)$ to $E(1111)$.

Functions $E(a0b0)$, $a \in \{-1, 0, 1\}$ represent rules with fixed upper boundary θ_2 of excitation and dynamically updated lower boundary θ_1 . These are equivalent to dynamically updated thresholds of excitation. Functions $E(0a0a)$, $a \in \{-1, 0, 1\}$ represent rules with fixed lower boundary and dynamical upper boundary of excitation interval.

The experiments are conducted on a cellular array of $n \times n$ cells with periodic boundary conditions. In a typical experiment we perturb resting cellular array with a localised domain of excitation, wait till transient period is over (1000 iterations is enough) and most excitation patterns collide and disappear and persist indefinitely, and then analyse

three configurations: configuration of excitation represented by an array of cells states x^t , and configurations of lower $\theta_1^t(x)$ and upper $\theta_2^t(x)$ boundaries of excitation intervals.

Initially $\theta_2^0(x) = 8$ for any x . In experiments we considered initial conditions $\theta_1^0(x) = 1$ and $\theta_1^0(x) = 2$. The following scenaria of initial excitation were played:

- $(++)$ -start, $\theta_1 = 2$: all cells are resting but two neighbouring cells are assigned excited state,
- R1-start: let D be a disc radius $n/4$ centred in the array L of $n \times n$ cells, all cells are resting but cells lying in D are assigned excited states with probability 0.2 and $\theta_1^0(x) = 1$ for any x ,
- R2-start: all cells are resting but cells lying in D get excited states with probability 0.2 and $\theta_1^0(x) = 2$ for any x ,
- D1-start: all cells are resting but cells lying in D get excited states with probability 0.1 or refractory states with probability 0.1 and $\theta_1^0(x) = 1$ for any x ,
- D2-start: all cells are resting but cells lying in D get excited states with probability 0.1 or refractory states with probability 0.1 and $\theta_1^0(x) = 2$ for any x ,
- $(-+)$ -start: all cells are resting but one cell is excited and its western neighbour is refractory,
- $(-++)$ -start all cells are resting but one cell is excited, its first order western neighbour is excited and its second order western neighbour is refractory.

Cell states were represented by colours and grey levels as follows: excited state $+$ is red (c. 76 grey), resting state is white and refractory state $-$ is blue (c. 28 grey). Colour values of excitation interval boundaries θ_1 and θ_2 are following: 1 is white, 2 is green or 150 grey, 3 is yellow or 226 grey, 4 is blue or 28 grey, 5 is magenta or 104 grey, 6 is cyan or 178 grey, 7 is red or 76 grey, and 8 is black.

3. MORPHOLOGICAL DIVERSITY

We evaluated morphological diversity of configurations of excitation and using Shannon entropy and Simpson's index. Let $W = \{o, +, -\}$ be a set of all possible configurations of a 9-cell neighbourhood $w(x) = u(x) \cup x$, $x \in \mathbf{L}$. Let c be a configuration of automaton, we calculate number of non-resting neighbourhood configurations as $\eta = \sum_{x \in \mathbf{L}} \epsilon(x)$, where $\epsilon(x) = 0$ if for every resting x all its neighbours are resting, and $\epsilon(x) = 1$ otherwise. The Shannon entropy is calculated as $\mathcal{E} = -\sum_{w \in W} (\nu(w)/\eta \cdot \ln(\nu(w)/\eta))$, where $\nu(w)$ is a number of times the neighbourhood configuration w is found in automaton configuration c . Simpson's index is calculated as $S = 1 - \sum_{w \in W} (\nu(w)/\eta)^2$. The measures \mathcal{E} and S were calculated on configurations of cell-states and interval boundaries after long transient period, sufficient enough for any perturbation to settle down.

The diversity of excitation patters is evaluated using S - \mathcal{E} plots. See examples of S - \mathcal{E} plots for D1-start, $\theta_1^0(x) = 1$, in Fig. 1 and $(++)$ -start, $\theta_1^0(x) = 2$, in Fig. 2. Distributions of functions by their values of Shannon entropies for θ_1 and θ_2 are illustrated in Figs. 3 and 4

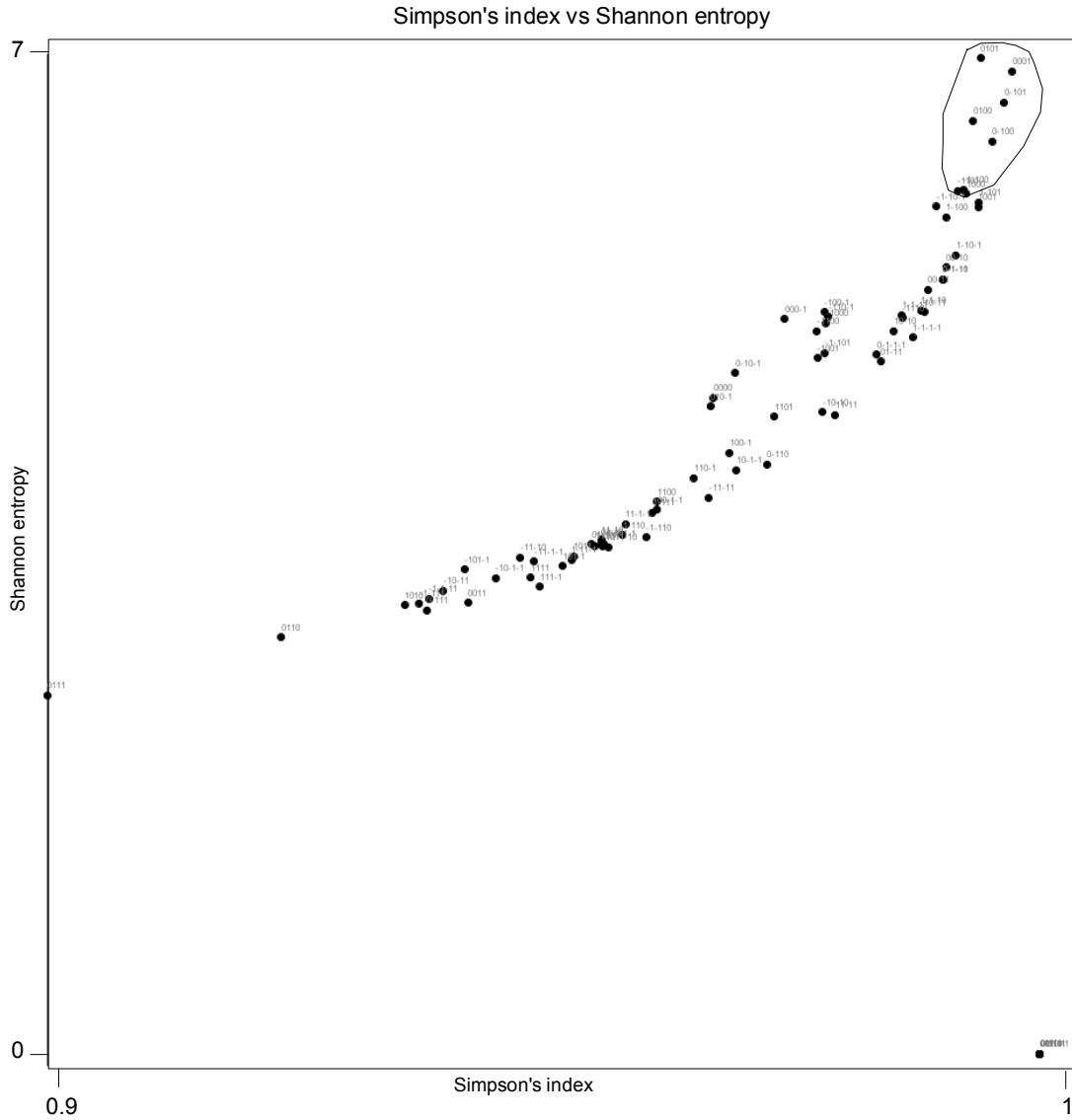


FIGURE 1. Morphological diversity of functions for D1-start, $\theta_1^0(x) = 1$ for all x : Simpson's index S (horizontal axis) vs Shannon entropy \mathcal{E} (vertical axis) for configuration of excitable array of 200×200 cells with periodic boundary condition, recorded at $t = 1000$. Encircled data points are seven functions with highest morphological diversity specified in column D1-start, S - \mathcal{E} in Tab. 3.

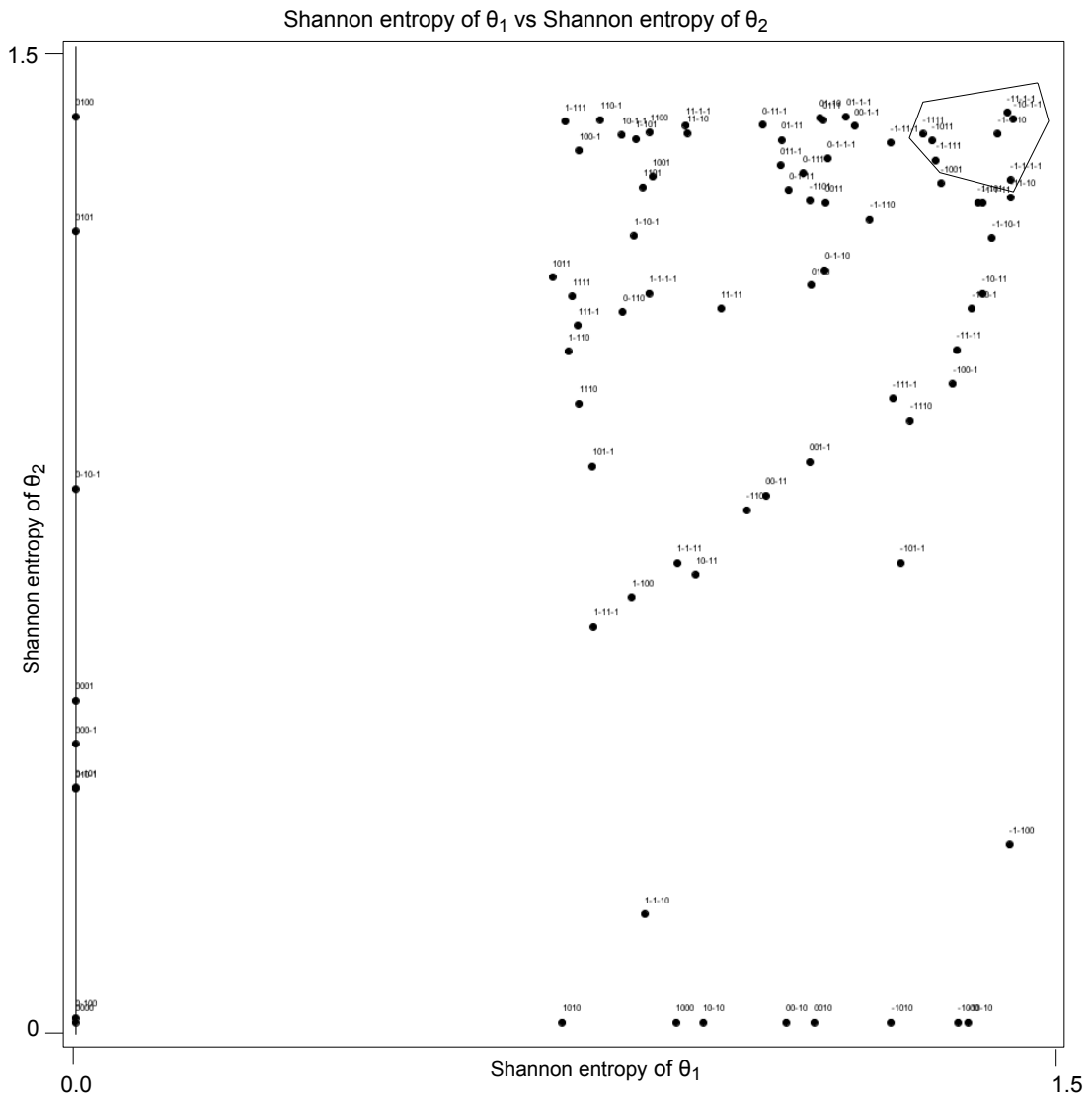


FIGURE 3. Morphological diversity of functions for D1-start, $\theta_1^0(x) = 1$ for all x : Shannon entropy \mathcal{E}_1 for configuration of θ_1 (horizontal axis) vs Shannon entropy \mathcal{E}_2 for configuration of θ_2 (vertical axis), recorded at $t = 1000$. Encircled data points are seven functions with highest morphological diversity specified in column D1-start, \mathcal{E}_1 - \mathcal{E}_2 in Tab. 3.

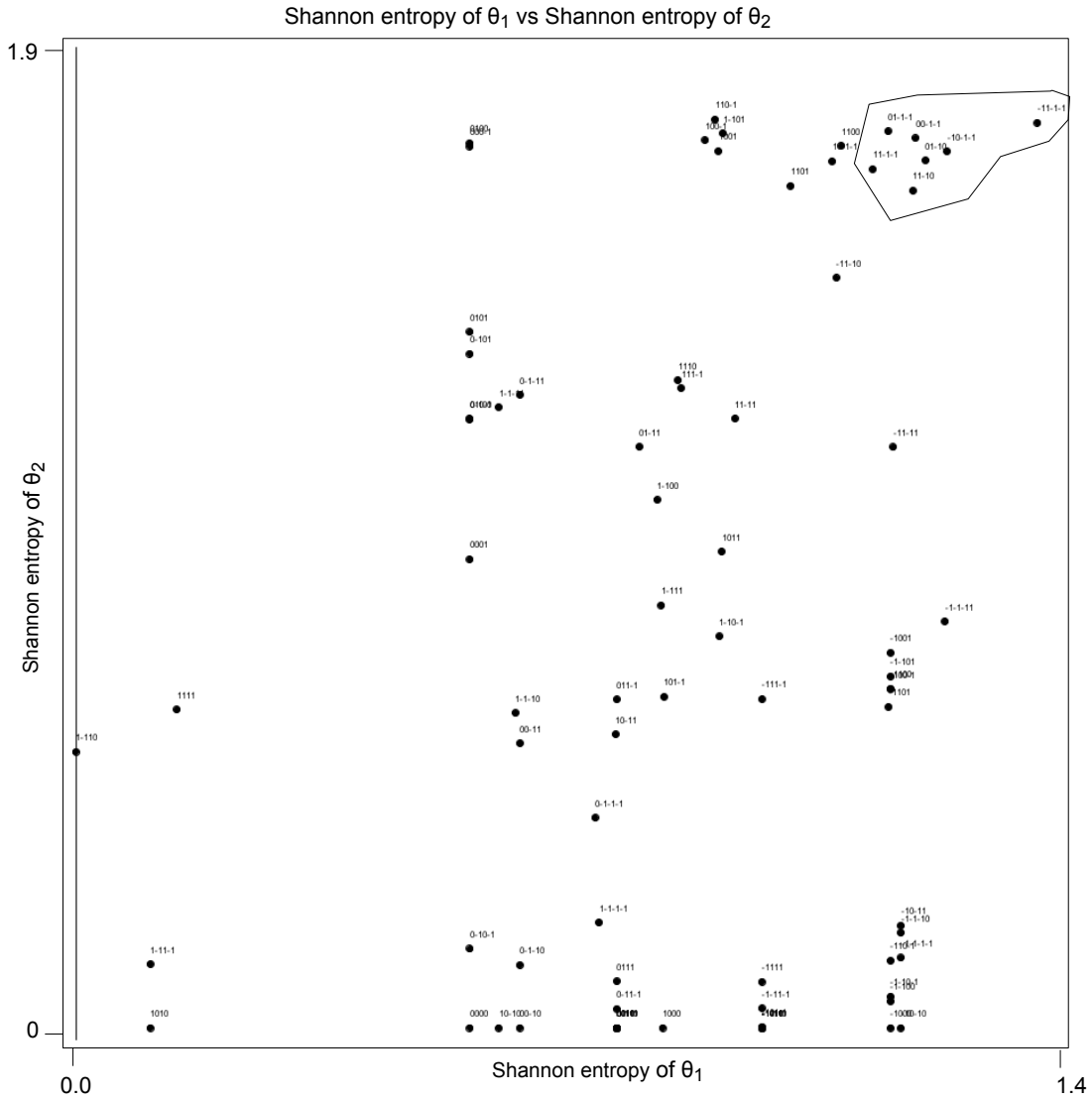


FIGURE 4. Morphological diversity of functions for $(++)$ -start, $\theta_1^0(x) = 2$ for all x : Shannon entropy \mathcal{E}_1 for configuration of θ_1 (horizontal axis) vs Shannon entropy \mathcal{E}_2 for configuration of θ_2 (vertical axis), recorded at $t = 1000$. Encircled data points are seven functions with highest morphological diversity specified in column $(++)$ -start, \mathcal{E}_1 - \mathcal{E}_2 in Tab. 3.

(++)-start, $\theta_2 = 2$		R1-start		R2-start		D1-start		D2-start		(-+)-start		(- + +)- start	
$S-\mathcal{E}$	$\mathcal{E}_1-\mathcal{E}_2$	$S-\mathcal{E}$	$\mathcal{E}_1-\mathcal{E}_2$	$S-\mathcal{E}$	$\mathcal{E}_1-\mathcal{E}_2$	$S-\mathcal{E}$	$\mathcal{E}_1-\mathcal{E}_2$	$S-\mathcal{E}$	$\mathcal{E}_1-\mathcal{E}_2$	$S-\mathcal{E}$	$\mathcal{E}_1-\mathcal{E}_2$	$S-\mathcal{E}$	$\mathcal{E}_1-\mathcal{E}_2$
<u>000-1</u>	-10-1-1		-1-1-11	-100-1	-1-1-1-1	0-100	-1-1-1-1	<u>0100</u>	-1-11-1	-1-100	-1-1-1-1	<u>000-1</u>	<u>1-101</u>
0100	<u>-11-1-1</u>		-11-11	<u>0100</u>	-1-1-1-1	0-101	-1-1-10	1-10-1	-1-110	0-1-1-1	-1-1-10	0100	100-1
1010	00-1-1		1-1-1-1	0101	-1-11-1	0001	<u>-1-101</u>	1-100	-1-111	0-100	-1-1-11	1-101	1001
11-10	01-1-1		1-1-11	1-10-1	-1-110	0100	-10-1-1	1-101	-10-1-1	0-101	<u>-1-101</u>	11-10	11-11
1100	01-10		1-11-1	1-100	-10-1-1	<u>0101</u>	-11-1-1	100-1	<u>-1011</u>	0001	-10-1-1	1100	<u>110-1</u>
1101	11-1-1		<u>1-111</u>	1000	<u>-1011</u>	1-100	1-1-11	1000	-11-1-1	1-101	-10-11	1101	111-1
1111	11-10		11-11	1101	-1111	1000	<u>11-1-1</u>	1101	-1111	1001	<u>-1001</u>	1111	1110

TABLE 1. Diversity of excitation is measured by selecting seven functions with highest values \mathcal{E} and S (columns $\mathcal{E}-S$) and diversity of excitation interval configuration by selecting seven functions with highest values \mathcal{E}_1 and \mathcal{E}_2 (columns $\mathcal{E}_1-\mathcal{E}_2$), i.e. Shannon entropy calculated on configurations of θ_1 and θ_2 . Functions exhibiting highest morphological diversity in their groups are underlined.

Top seven functions showing highest values of diversity indices, e.g. those encircled in examples Fig. 1–4, are grouped in Tab. 3 for various scenarios of initial start.

Finding 1. *There is no match between functions which produce configurations of excitation with highest morphological diversity and configurations of interval boundaries with highest morphological diversity.*

Amongst functions listed in Tab. 3 only function $E(1 - 101)$ gets into top seven functions with highest diversity of both excitation and interval boundaries for scenario $(- + +)$ -start. Exemplar configurations of excitation and interval boundaries generated by automaton governed by $E(1 - 101)$ are shown in Fig. 10b. Function $E(1 - 101)$ is also amongst functions with highest diversity for $D2$ - and $(- +)$ -start. The function governs the following update of the excitation interval boundaries. Low boundary $\theta_1(x)$ of excitation of cell x is updated only cell x is excited. The boundary $\theta_1(x)$ increases if cell x has more excited neighbours than refractory neighbours, $\theta_1(x)$ decreases if number of refractory neighbours of x exceeds number of excited neighbours. The boundary $\theta_1(x)$ does not change if cell x has the same number of excited neighbours as refractory neighbours. Upper boundary $\theta_2(x)$ increases if cell x 's dissents with excitation-refractoriness ratio in its neighbourhood: $x^t = +$ and $\sigma_+^t(x) < \sigma_-^t(x)$ or $x^t = -$ and $\sigma_+^t(x) > \sigma_-^t(x)$. The boundary $\theta_2(x)$ decreases if cell x conforms to excitation-refractoriness ratio in its neighbourhood: $x^t = +$ and $\sigma_+^t(x) > \sigma_-^t(x)$ or $x^t = -$ and $\sigma_+^t(x) < \sigma_-^t(x)$. Increase of θ_1 and decrease of θ_2 lead to decrease cell's excitability. Thus we can characterise function $E(1 - 101)$ as follows: excitability of a cell decreases if the cell dissents with its neighbourhood and increases otherwise.

Finding 2. *Functions $E(-1 - 101)$ and $E(-1011)$ generate configurations of excitation interval boundaries with highest morphological diversity for three and two types of initial stimulation, respectively, and functions $E(000 - 1)$ and $E(0100)$ generate configurations of excitation with highest morphological diversity for two types of initial stimulation.*

The function $E(-1 - 101)$ generates configurations with highest morphological diversity of θ_1 and θ_2 configurations for $R2$ -, $D1$ - and $(- +)$ -starts, see examples in Fig. 7b and 9b, and $E(-1011)$ generates highest morphological diversity configurations of θ_1 and θ_2 for $R2$ - and $D2$ -starts (Figs. 6b and 8b). The functions $E(000 - 1)$ and $E(0100)$ produce highest morphological diversity configurations of excitation for $(++)$ - and $(-- +)$ -starts ($E(000 - 1)$) and $R2$ - and $D2$ -starts ($E(0100)$). See examples for $E(000 - 1)$ in Figs. 5a and 10a and $E(0100)$ in Figs. 6a and 8a.

Finding 3. *Function $E(0100)$ generates most morphologically diverse excitation patterns in larger, comparing to other functions, number of initial conditions.*

Function $E(0100)$ is amongst top seven functions with highest morphological diversity of excitation in $(++)$ -, $R2$ -, $D1$ -, $D2$ - and $(- + +)$ -starts (Tab. 3). The function generates most morphologically diverse excitations in $D2$ -start. Examples of configurations generated by $E(0100)$ are shown in Figs. 6a and 8a. The function $E(0100)$ shows how dynamics of excitation can be tuned by changing only upper boundary of the excitation interval with lower boundary fixed. Value $\theta_1(x)$ is not updated. Value $\theta_2(x)$ increases if cell x is excited and it has more excited than refractory neighbours, the value $\theta_2(x)$

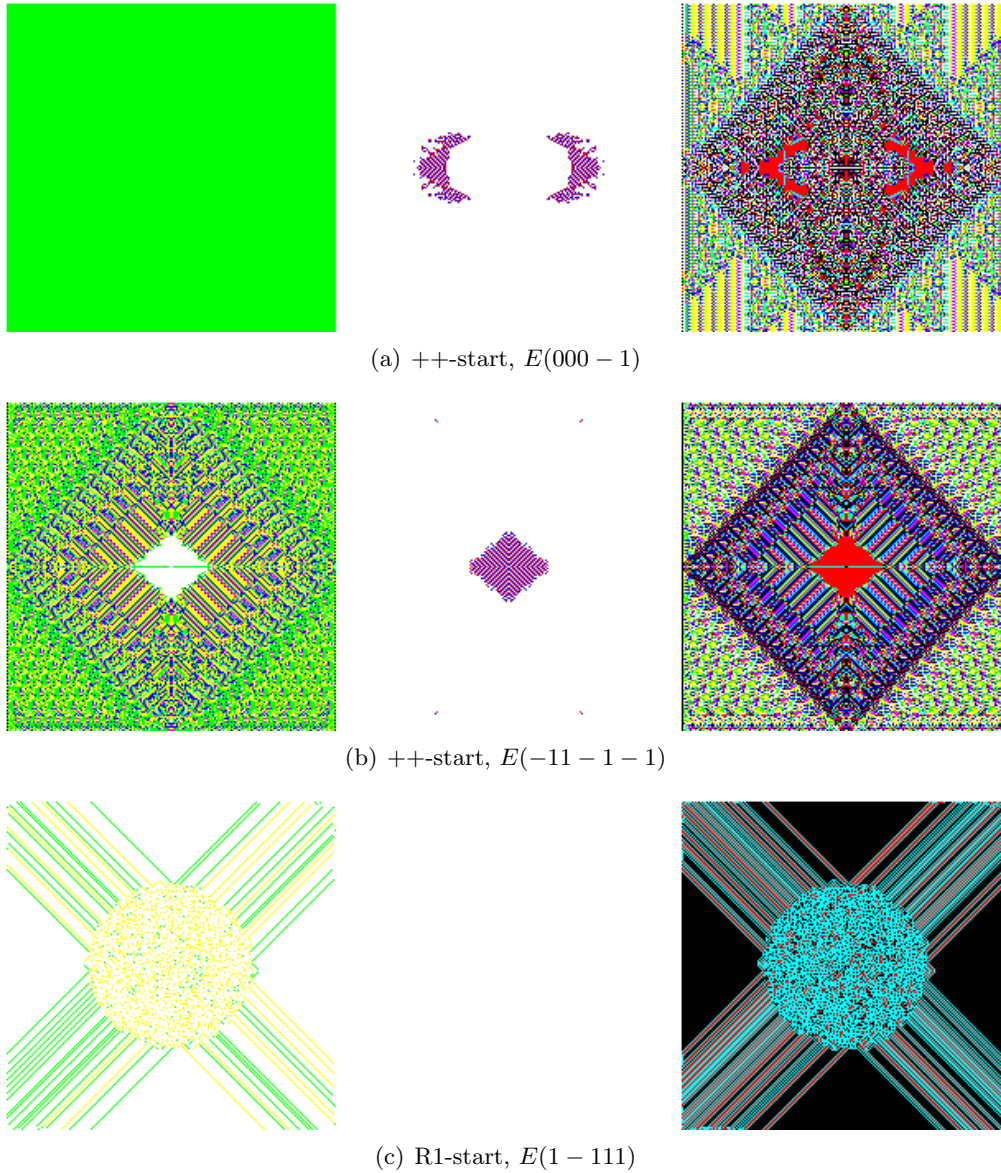


FIGURE 5. Examples of most morphologically diverse configurations generated in $(++)$ -start (ab) and R1-start (c). (a) Configurations with highest morphological diversity of excitation generated by function $E(000-1)$. (b) Configurations with highest morphological diversity of interval boundaries θ_1 and θ_2 generated by function $E(-11-1-1)$. (c) Configurations with highest morphological diversity of interval boundaries θ_1 and θ_2 generated by function $E(1-111)$. Configurations of θ_1 (left), excitation (middle) and θ_2 (right) are taken in 200×200 cell array, at $t = 1000$.

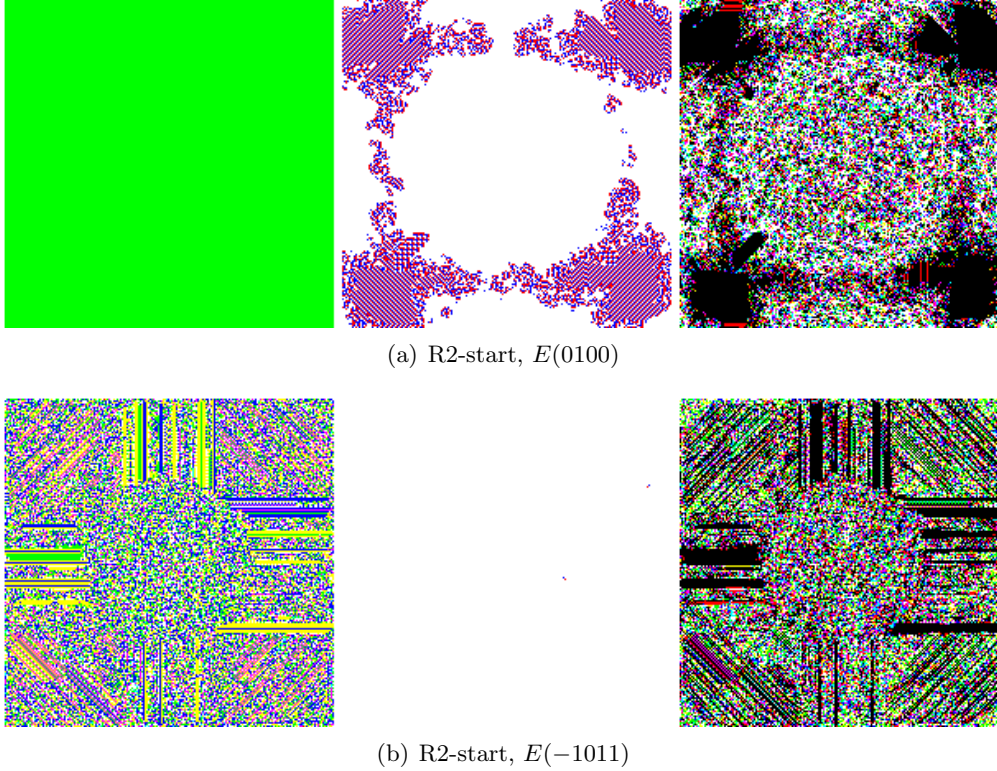


FIGURE 6. Examples of most morphologically diverse configurations generated in R2-start. (a) Configurations with highest morphological diversity of excitation generated by function $E(0100)$. (b) Configurations with highest morphological diversity of interval boundaries θ_1 and θ_2 generated by function $E(-1011)$. Configurations of θ_1 (left), excitation (middle) and θ_2 (right) are taken in 200×200 cell array, at $t = 1000$.

decreases if cell x is excited and has more refractory than excited neighbours. Excitability of a cell decreases if the cell dissents with excitation ratio in its neighbourhood, and increases otherwise.

Finding 4. *Function $E(-10-1-1)$ generates most morphologically diverse patterns of interval boundaries in larger, comparing to other functions, number of initial conditions.*

Function $E(-10-1-1)$ gets in top seven functions with highest morphological diversity of θ_1 and θ_2 patterns in $(++)$ -, R2-, D1-, D2-, and $(-+)$ -starts (Tab. 3). In automata, governed by this function, $\theta_2(x)$ is not updated if cell x is excited. Otherwise, $\theta_1(x)$ and $\theta_2(x)$ increase if refractory neighbours outnumber in the cell x 's neighbourhood and decrease if excited neighbours outnumber refractory neighbours.

Finding 5. *Upper boundary of excitation interval more significantly affects morphological diversity of configurations generated than lower boundary of the interval does.*

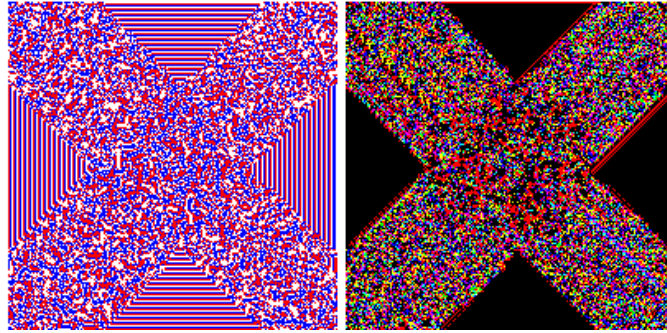
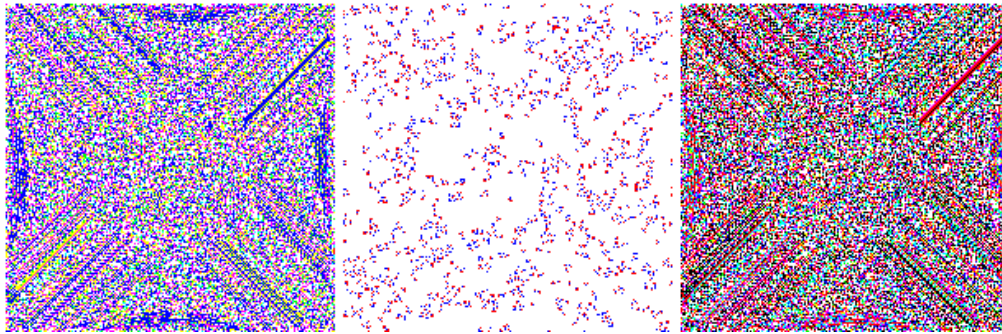
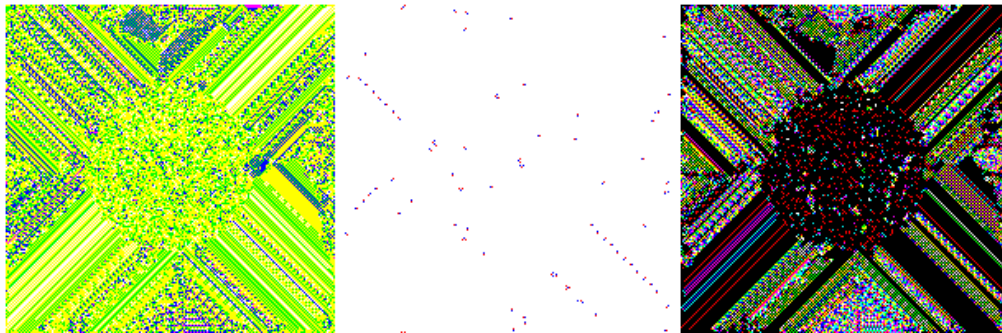
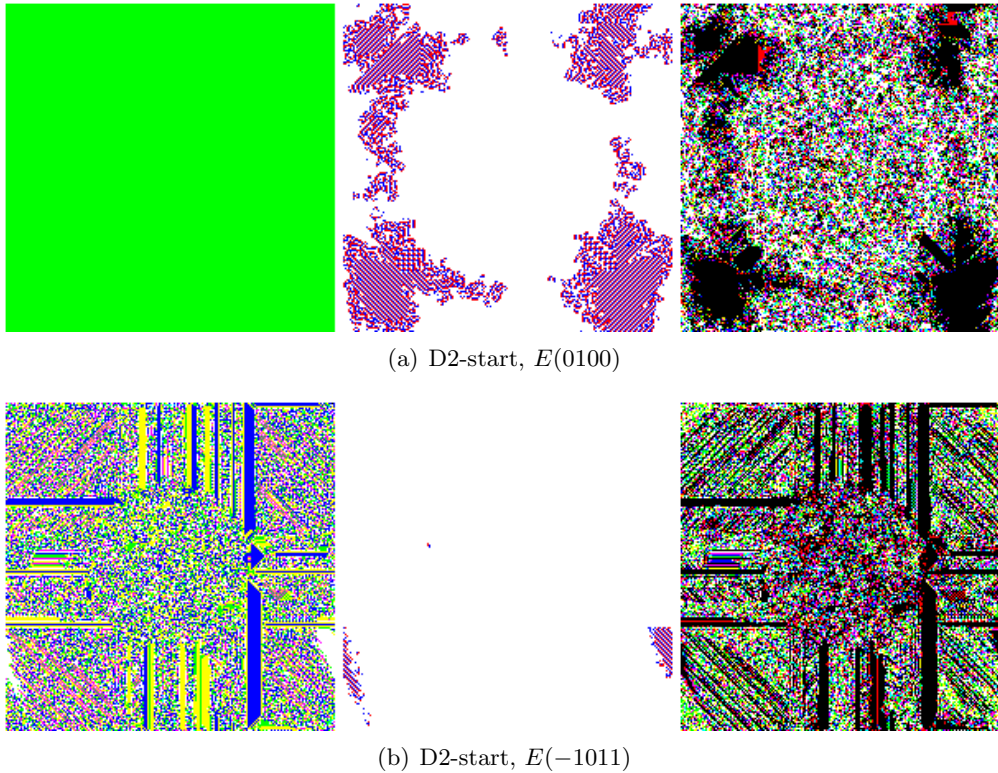
(a) D1-start, $E(0101)$ (b) D1-start, $E(-1 - 101)$ (c) D1-start, $E(11 - 1 - 1)$

FIGURE 7. Examples of most morphologically diverse configurations generated in D1-start. (a) Configurations with highest morphological diversity of excitation generated by function $E(0101)$. (b) Configurations with highest morphological diversity of interval boundaries θ_1 and θ_2 generated by function $E(-1 - 101)$. (c) Configurations with highest morphological diversity of interval boundaries θ_1 and θ_2 generated by function $E(11 - 1 - 1)$. Configurations of θ_1 (left), excitation (middle) and θ_2 (right) are taken in 200×200 cell array, at $t = 1000$.


 (a) D2-start, $E(0100)$

 (b) D2-start, $E(-1011)$

FIGURE 8. Examples of most morphologically diverse configurations generated in D2-start. (a) Configurations with highest morphological diversity of excitation generated by function $E(0100)$. (b) Configurations with highest morphological diversity of interval boundaries θ_1 and θ_2 generated by function $E(-1011)$. Configurations of θ_1 (left), excitation (middle) and θ_2 (right) are taken in 200×200 cell array, at $t = 1000$.

There are only two functions, $E(1010)$ and $E(1000)$, where only lower boundary θ_1 is updated in Tab. 3. Function $E(1010)$ represents a situation when $\theta_1(x)$ is independently of a state of cell x : $\theta_1(x)$ increases if number of excited neighbours exceeds number of refractory neighbours, and $\theta_1(x)$ decreases if refractory neighbours outnumber excited neighbours. In automata governed by function $E(1000)$ value of $\theta_1(x)$ is updated as above but only if cell x is excited. There are several functions with highest morphological diversity which represent fixed lower boundary and dynamical upper boundary, e.g. $E(000-1)$ (Figs. 5a and 10a), $E(0100)$ (Figs. 6a and 8a), $E(0101)$ (Fig. 7a), $E(0-100)$, $E(0-101)$, and $E(0001)$ (Tab. 3).

4. GENERATIVE DIVERSITY AND LOCALISATIONS

Generative diversity characterises how many different configurations are generated during space-time development of automaton starting with entirely resting configuration but single cell in a non-resting state. We consider two starting conditions: $(++)$ -start

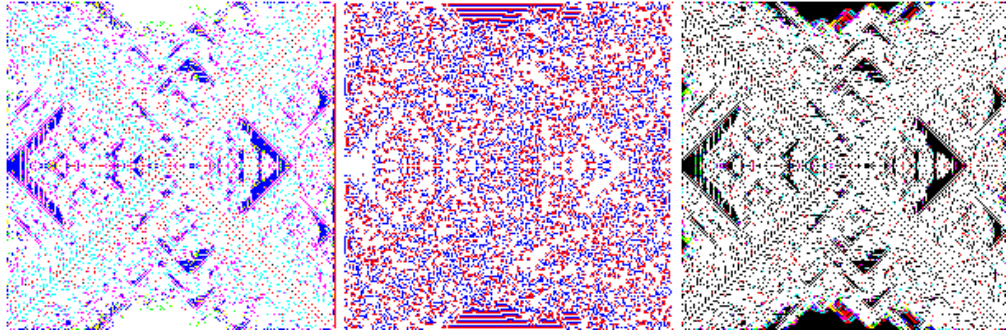
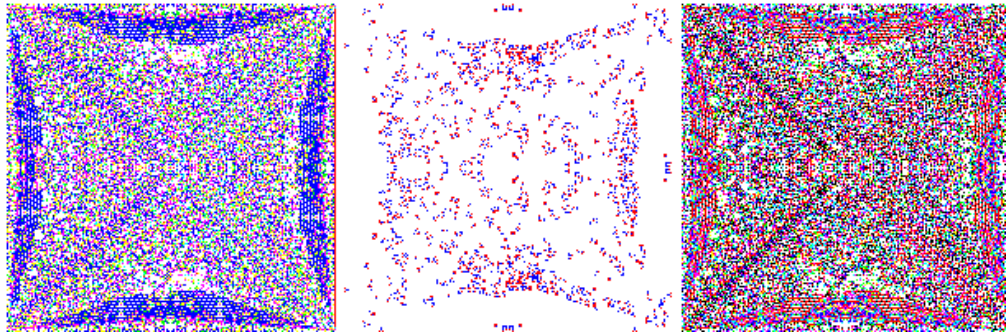
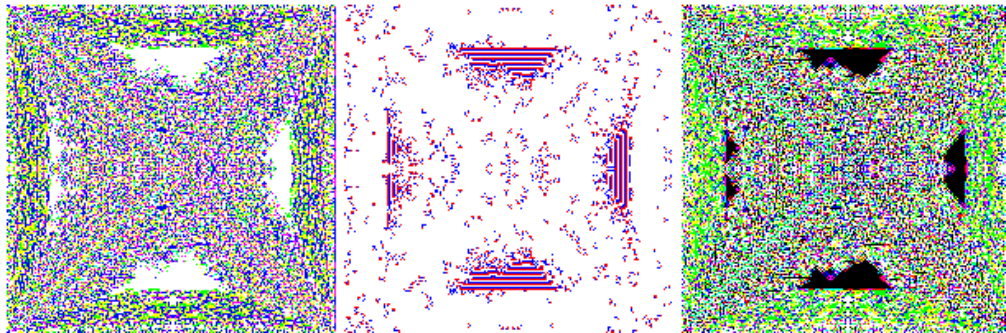
(a) $(-+)$ -start, $E(-1-100)$ (b) $(-+)$ -start, $E(-1-101)$ (c) $(-+)$ -start, $E(-1001)$

FIGURE 9. Examples of most morphologically diverse configurations generated in $(-+)$ -start. (a) Configurations with highest morphological diversity of excitation generated by function $E(-1-100)$. (b) Configurations with highest morphological diversity of interval boundaries θ_1 and θ_2 generated by function $E(-1-101)$. (c) Configurations with highest morphological diversity of interval boundaries θ_1 and θ_2 generated by function $E(-1001)$. Configurations of θ_1 (left), excitation (middle) and θ_2 (right) are taken in 200×200 cell array, at $t = 1000$.

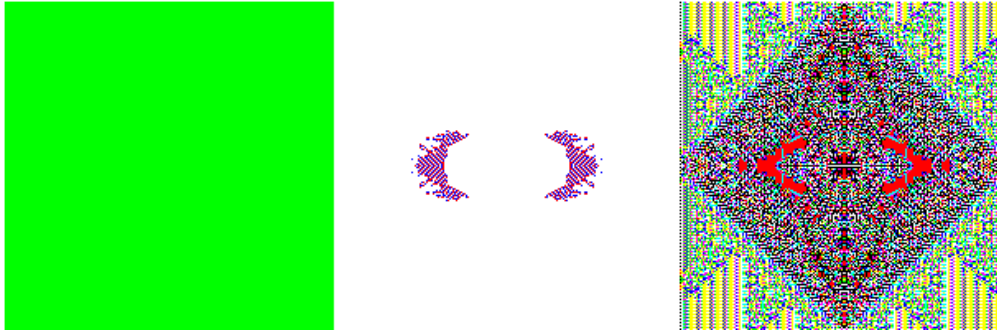
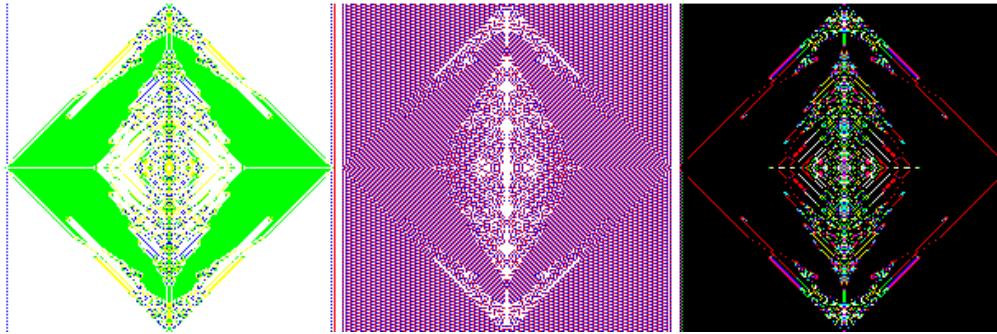
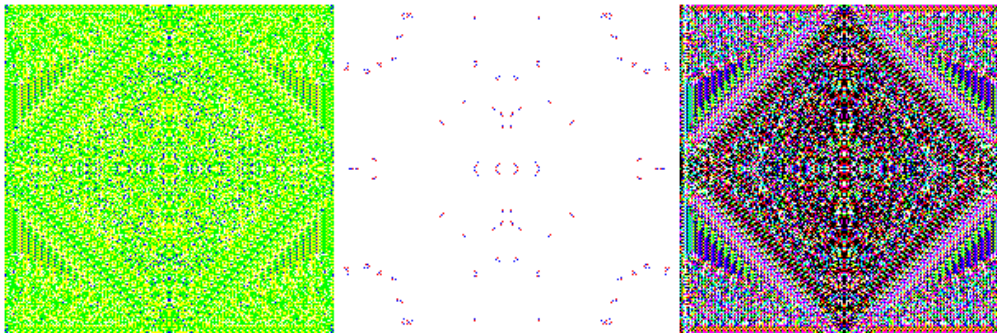

 (a) $(-++)$ -start, $E(000-1)$

 (b) $(-++)$ -start, $E(1-101)$

 (c) $(-++)$ -start, $E(110-1)$

FIGURE 10. Examples of most morphologically diverse configurations generated in $(-++)$ -start. (a) Configurations with highest morphological diversity of excitation generated by function $E(000-1)$. (b) Configurations with highest morphological diversity of interval boundaries θ_1 and θ_2 generated by function $E(1-101)$. (c) Configurations with highest morphological diversity of interval boundaries θ_1 and θ_2 generated by function $E(110-1)$. Configurations of θ_1 (left), excitation (middle) and θ_2 (right) are taken in 200×200 cell array, at $t = 1000$.

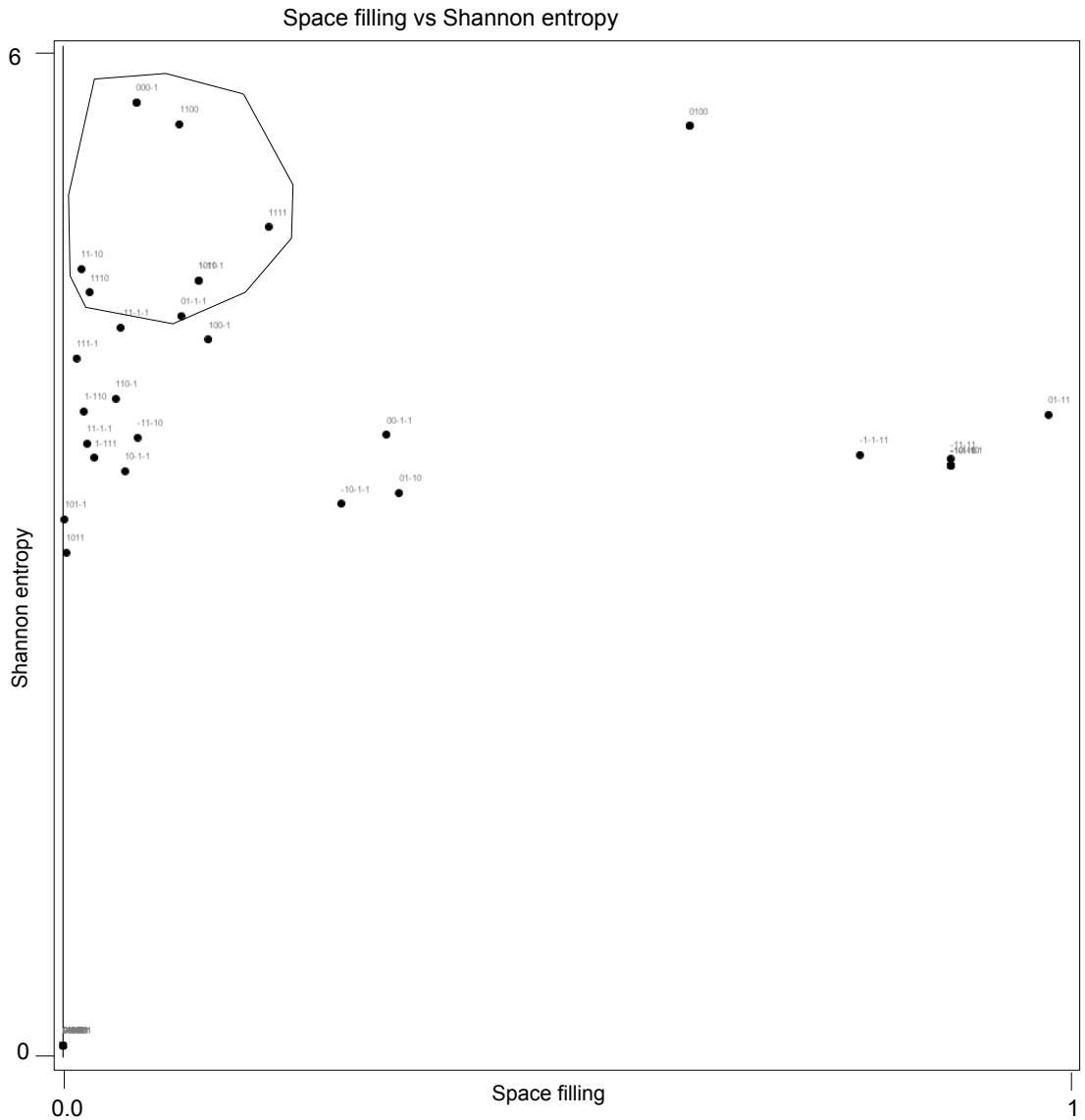


FIGURE 11. Generative diversity of functions for $(++)$ -start, $\theta_1^0(x) = 2$ for all x : Space filling (horizontal axis) vs Shannon entropy (vertical axis) for configuration of excitable array of 200×200 cells with periodic boundary condition, recorded at $t = 1000$. Encircled data points are seven functions with highest generative diversity specified in column $(++)$ -start, in Tab. 2.

and $\theta_1^0(x) = 2$ for any x ; $(-+)$ -start and $\theta_1^0(x) = 1$; and, $(--)$ -start and $\theta_1^0(x) = 2$. Generative diversity is evaluated using Shannon entropy and space-filling (a ratio of cells in a non-resting state). Functions generating configurations with maximum Shannon

(++)- and (- + +)-start, $\theta_1^0 = 2$	(-+)-start, $\theta_1^0 = 1$
-11 - 1 - 1	-1 - 101
01 - 1 - 1	0 - 1 - 1 - 1
100 - 1	00 - 1 - 1
1010	01 - 1 - 1
11 - 10	01 - 11
1110	10 - 1 - 1
1111	11 - 11

TABLE 2. Seven functions with highest generative diversity for (++)- and (- + +)-start, $\theta_1 = 2$ (first column) and (-+)-start, $\theta_1 = 1$ (second column).

(++)-start	(-+)-start
10 - 1 - 1	-10 - 1 - 1
11 - 1 - 1	-11 - 10
11 - 10	00 - 1 - 1
100 - 1	01 - 1 - 1
101 - 1	01 - 10
110 - 1	10 - 1 - 1
111 - 1	11 - 1 - 1
1011	11 - 10
1110	

TABLE 3. Functions supporting localizations in (++)- and (- + +)-start (left column) and (-+)-start (right column).

entropy and minimum space-filling are assumed to have higher generative complexity, see example in Fig. 12.

Seven functions with highest generative diversity are listed in Tab. 2. Configurations of excitation and interval boundaries for $E(-11 - 1 - 1)$, ++-start, shown in Fig. 5b, $E(-1 - 101)$, (-+)-start, in Fig. 9b and configurations generated by functions $E(1111)$, $E(11 - 10)$ and $E(0 - 1 - 1 - 1)$ in Fig. 12.

Finding 6. *Most localizations generated in (++)- and (- + +)-starts are stationary.*

Around half of the functions generate configurations with localizations in case of R2-start (43), D1-start (41), D2-start (43). We concentrate on functions which produce localizations in singleton starts. There nine functions for (++)- and eight function for (-+)-start, $\theta_1^0 = 2$ (Tab. 3). Examples of configurations generated by functions $E(00 - 1 - 1)$, $E(101 - 1)$, $E(1110)$ and $E(00 - 1 - 1)$ are shown in Fig. 13.

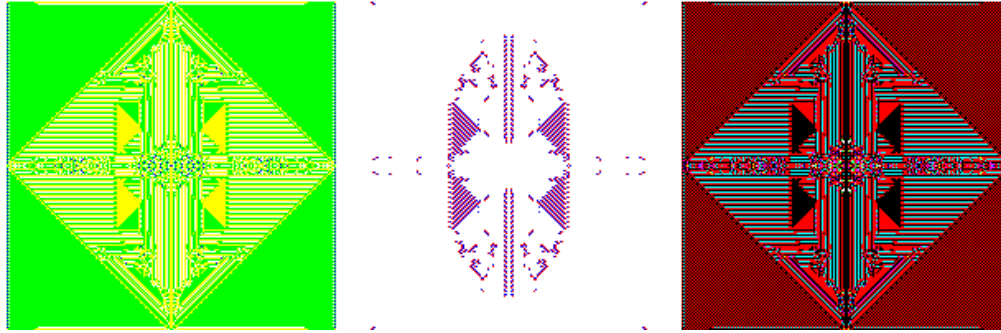
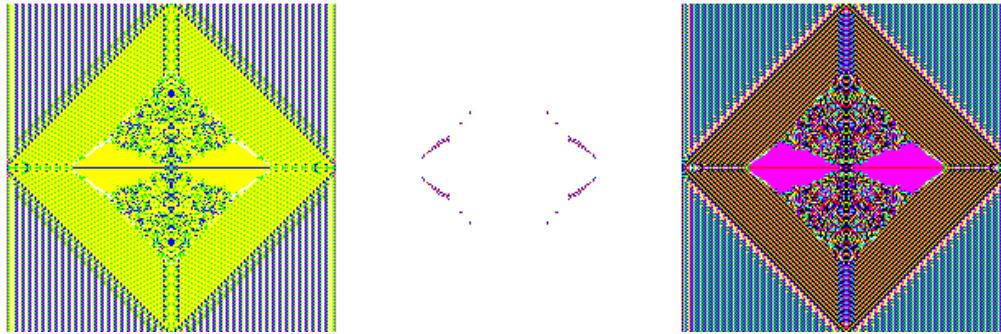
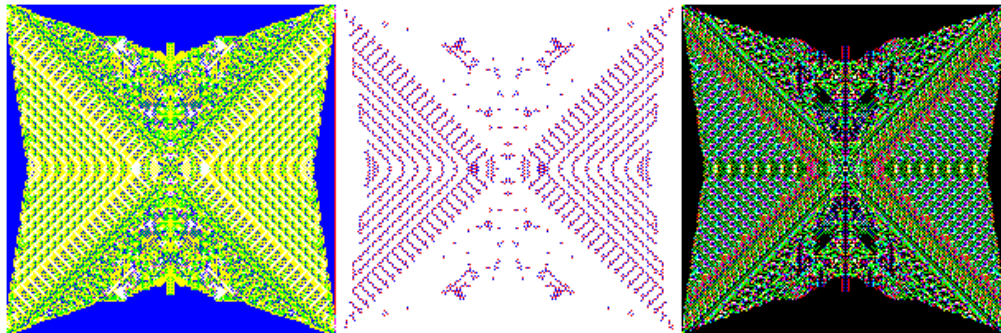
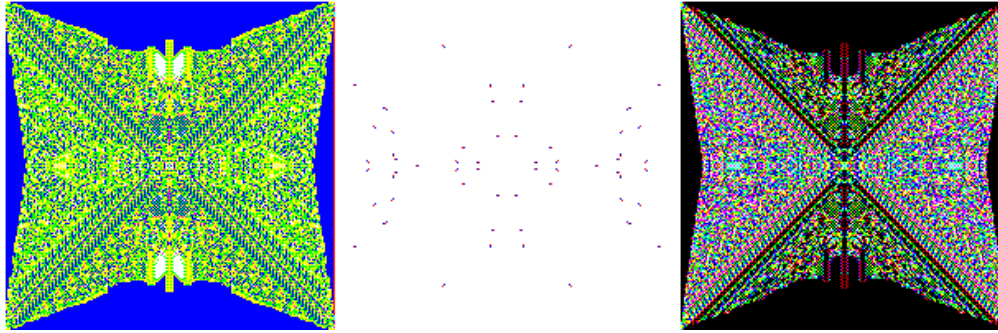
(a) $(++)$ -start, $\theta_1^0 = 2$, $E(1111)$ (b) $(++)$ -start, $\theta_1^0 = 2$, $E(11-10)$ (c) $(-+)$ -start, $\theta_1^0 = 1$, $E(0-1-1-1)$

FIGURE 12. Examples of configurations generated by functions with highest generative diversity. (a) $E(1111)$, (b) $E(11-10)$, (c) $E(0-1-1-1)$. Automaton array has 200×200 cells, configurations of θ_1 (left), excitation (middle) and θ_2 (right) at $t = 1000$.

Finding 7. *Functions $E(11-10)$ and $100-1$ are amongst top seven functions with highest generative diversity supporting localised excitation dynamics in scenarios of $(++)$ -start. Functions $E(00-1-1)$, $E(01-1-1)$, $E(10-1-1)$ and $E(11-1-1)$ are amongst top seven functions with highest generative diversity supporting localised excitation dynamics in scenarios of $(-+)$ -start*


 (a) $(++)$ -start, $\theta_1^0 = 2$, $E(00 - 1 - 1)$

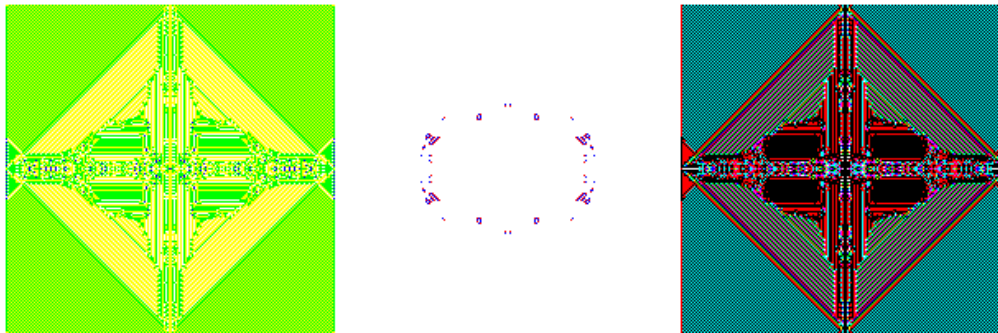
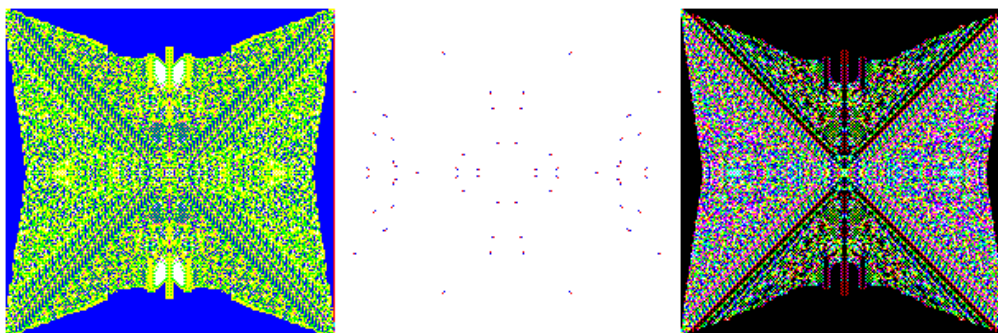
 (b) $(++)$ -start, $\theta_1^0 = 2$, $E(101 - 1)$

 (c) $(++)$ -start, $\theta_1^0 = 2$, $E(1110)$

 (d) $(-+)$ -start, $\theta_1^0 = 1$, $E(00 - 1 - 1)$

FIGURE 13. Examples of configurations with localised excitations developed in $(++)$ -start (abc) and $(-+)$ -start (d) scenarios. Size of cellular array is 200×200 cells, configurations of θ_1 (left), excitation (middle) and θ_2 (right) at $t = 1000$.

See Tabs. 2 and 3. Configurations generated by function $E(11 - 10)$ are exemplified in Fig. 12b and function $E(00 - 1 - 1)$ in Fig. 13a. Functions $E(100 - 1)$ and $E(00 - 1 - 1)$ are the functions with minimal updates of excitation interval boundaries. In automata governed by function $E(00 - 1 - 1)$ $\theta_1(x)$ and $\theta_2(x)$ are updated only if the cell x is in refractory state: both boundaries decrease if excited neighbours of x outnumber refractory neighbours, and they increase if refractory neighbours dominate. In automata governed by function $E(100 - 1)$ the boundary $\theta_1(x)$ increases if the excited cell x has more excited neighbours than refractory ones, and boundary and decreases if the cell has more refractory neighbours. The boundary $\theta_2(x)$ is updated only if cell x is refractory: $\theta_2(x)$ decreases if excited neighbours outnumber refractory neighbours, and it increases otherwise.

5. SUMMARY

Excitable cellular automata with dynamical excitation interval exhibit a wide range of space-time dynamics based on an interplay between propagating excitation patterns which modify excitability of the automaton cells. Such interactions leads to formation of standing domains of excitation, stationary waves and localised excitations. We analysed morphological and generative diversities of the functions studied and characterised the functions with highest values of the diversities. Amongst other intriguing discoveries we found that upper boundary of excitation interval more significantly affects morphological diversity of configurations generated than lower boundary of the interval does and there is no match between functions which produce configurations of excitation with highest morphological diversity and configurations of interval boundaries with highest morphological diversity. Potential directions of futures studies of excitable media with dynamically changing excitability may focus on relations of the automaton model with living excitable media, e.g. neural tissue and muscles, and novel materials with memristive properties, and networks of conductive polymers.

REFERENCES

- [1] Adamatzky A. and Holland O. Phenomenology of excitation in 2D cellular automata and swarm systems. *Chaos, Solitons & Fractals* 3 (1998) 1233–1265.
- [2] Adamatzky A., De Lacy Costello B., Asai T. *Reaction-Diffusion Computers* (Elsevier, Amsterdam, New York, 2005).
- [3] Chopard B. and Droz M. *Cellular Automata Modeling of Physical Systems* (Cambridge University Press, 2005).
- [4] Gerhardt M., Schuster H. and Tyson J. J. A cellular excitable media. *Physica D* 46 (1990) 392–415.
- [5] Greenberg J. M. and Hastings S. P. Spatial patterns for discrete models of diffusion in excitable media, *SIAM Journal on Applied Mathematics* 34 (1978) 515–523.
- [6] Hartman H. and Tamayo P., Reversible cellular automata and chemical turbulence, *Physica D* 45 (1990) 293–306.
- [7] Ilachinski A. *Cellular Automata: A Discrete University* (World Scientific, Singapore, 2001).
- [8] Markus M. and Hess B. Isotropic cellular automata for modelling excitable media. *Nature* 347 (1990) 56–58.
- [9] Yaguma S., Odagir K. and Takatsuka K. Coupled-cellular-automata study on stochastic and pattern-formation dynamics under spatiotemporal fluctuation of temperature. *Physica D* 197 (2004) 34–62.
- [10] Yang X. Pattern formation in enzyme inhibition and co-operativity with parallel cellular automata. *Parallel Computing* 30 (2004) 741–751.

- [11] Yang X. Computational modelling of nonlinear calcium waves. *Appl. Mathem. Modelling* 30 (2006) 200–208.
- [12] Young D. A local activator–inhibitor model of vertebrate skin patterns. *Math. Biosci.* 72 (1984) 51–58.

(Adamatzky) UNIVERSITY OF THE WEST OF ENGLAND, BRISTOL, UK
E-mail address: `andrew.adamatzky@uwe.ac.uk`